Naval Surface Warfare Center
Carderock Division
West Bethesda, MD 20817-5700

Numerical Simulation of Gleeble Torsion Testing of HSLA-65 Steel

by

David R. Forrest and Matthew F. Sinfield

Naval Surface Warfare Center
Carderock Division
West Bethesda, MD 20817-5700

Numerical Simulation of Gleeble Torsion Testing of HSLA-65 Steel

by

David R. Forrest and Matthew F. Sinfield

REPORT DOCUMENTATION PAGE

Form Approved
OMB No. 0704-0188

Public reporting burden for this collection of information is estimated to average 1 hour per response, including the time for reviewing instructions, searching existing data sources, gathering and maintaining the data needed, and completing and reviewing this collection of information. Send comments regarding this burden estimate or any other aspect of this collection of information, including suggestions for reducing this burden to Department of Defense, Washington Headquarters Services, Directorate for Information Operations and Reports (0704-0188), 1215 Jefferson Davis Highway, Suite 1204, Arlington, VA 22202-4302. Respondents should be aware that notwithstanding any other provision of law, no person shall be subject to any penalty for failing to comply with a collection of information if it does not display a currently valid OMB control number. **PLEASE DO NOT RETURN YOUR FORM TO THE ABOVE ADDRESS.**

1. REPORT DATE *(DD-MM-YYYY)* 01-04-2008	2. REPORT TYPE FINAL	3. DATES COVERED *(From - To)*
4. TITLE AND SUBTITLE Numerical Simulation of Gleeble Torsion Testing of HSLA-65 Steel		5a. CONTRACT NUMBER
		5b. GRANT NUMBER
		5c. PROGRAM ELEMENT NUMBER
6. AUTHOR(S) David R. Forrest and Matthew F. Sinfield		5d. PROJECT NUMBER
		5e. TASK NUMBER
		5f. WORK UNIT NUMBER 08-1-6110-958
7. PERFORMING ORGANIZATION NAME(S) AND ADDRESS(ES) AND ADDRESS(ES) NAVAL SURFACE WARFARE CENTER CARDEROCK DIVISION (CODE 6110) 9500 MACARTHUR BLVD WEST BETHESDA MD 20817-5700		8. PERFORMING ORGANIZATION REPORT NUMBER NSWCCD-61-TR-2008/02
9. SPONSORING / MONITORING AGENCY NAME(S) AND ADDRESS(ES)		10. SPONSOR/MONITOR'S ACRONYM(S)
		11. SPONSOR/MONITOR'S REPORT NOS

12. DISTRIBUTION / AVAILABILITY STATEMENT
Approved for public release; distribution is unlimited.

13. SUPPLEMENTARY NOTES

14. ABSTRACT

NSWCCD has used a Gleeble thermomechanical simulator as a tool to provide carefully controlled deformation cycles on metallurgical samples to study the properties and physics of friction stir welds. Our Gleeble experiments provide critical information that cannot be obtained from experimental friction stir welds because the metallurgical state can change radically with position due to the extreme thermal and strain field gradients within a friction stir weld. This allows us to independently vary strain and temperature with time in ways that may not even be possible under normal friction stir welding conditions.

NSWCCD is now analyzing Gleeble torsion samples as part of an ILIR project to gain a fundamental understanding of microstructural evolution during friction stir welding of HSLA-65 steel for Naval applications.

NSWCCD developed a numerical model of the Gleeble torsion test to predict the deformation behavior of a specimen to a high degree of fidelity, and provide detailed quantitative information about the strain, strain rate, and temperature history with time throughout the volume of the specimen. The numerical model was necessary to determine the complex thermomechanical distribution within the sample in order to interpret the test results. This numerical model is being used as part of the continuing ILIR project to relate different torsion sample microstructures and properties to their actual thermomechanical histories for comparison with actual friction stir welds.

We now have a material model for the high temperature deformation of HSLA-65 that can be used for future DEFORM simulations.

15. SUBJECT TERMS
Numerical Simulation; Gleeble Torsion Testing; HSLA-65 Steel

16. SECURITY CLASSIFICATION OF:			17. LIMITATION OF ABSTRACT	18. NUMBER OF PAGES	19a. NAME OF RESPONSIBLE PERSON David R. Forrest
a. REPORT UNCLASSIFIED	b. ABSTRACT UNCLASSIFIED	c. THIS PAGE UNCLASSIFIED	SAR	36	19b. TELEPHONE NUMBER *(include area code)* 301-227-5033

This page intentionally left blank

Table of Contents

<div align="right">Page</div>

Figures

Tables

Administrative Information

Acknowledgements

This page intentionally left blank

Executive Summary

For several years now, we have used a Gleeble thermomechanical simulator as a tool to provide carefully controlled deformation cycles on metallurgical samples in order to study the properties and physics of friction stir welds. The Gleeble experiments provide critical information that cannot be obtained from experimental friction stir welds: although we can analyze material from a friction stir weld, we do not know the detailed thermomechanical history at specific points within a weld. This is because the metallurgical state can change radically with position due to the extreme thermal and strain field gradients within a friction stir weld. By contrast, the Gleeble allows us to generate a larger test volume of material with a known thermomechanical history that we can evaluate. Furthermore, it allows us to independently vary strain and temperature with time in ways that may not even be possible under normal friction stir welding conditions.

At Ohio State University Matthew Sinfield's master's thesis work involved the use of a Gleeble 3800 Torsion machine on HSLA-65 steel to simulate the friction stir welding of this material. We are now analyzing those same OSU Gleeble torsion samples as part of an ILIR project to gain a fundamental understanding of microstructural evolution during friction stir welding of HSLA-65 steel for Naval applications.

We developed a numerical model of the Gleeble torsion test to predict the deformation behavior of a specimen to a high degree of fidelity, and provide detailed quantitative information about the strain, strain rate, and temperature history with time throughout the volume of the specimen. The numerical model was necessary to determine the complex thermomechanical distribution within the sample in order to interpret the test results. This numerical model is being used as part of the continuing ILIR project to relate different torsion sample microstructures and properties to their actual thermomechanical histories for comparison with actual friction stir welds.

Another benefit of this work is that we now have a material model for the high temperature deformation of HSLA-65 that can be used for future DEFORM simulations. For example, we can use DEFORM 3D to model the friction stir welding process itself, accounting for many of the physical effects that are not taken into account by our current friction stir model.

Introduction

For several years now, we have used a Gleeble thermomechanical simulator as a tool to provide carefully controlled deformation cycles on metallurgical samples in order to study the properties and physics of friction stir welds [1-5]. The Gleeble experiments provide critical information that cannot be obtained from experimental friction stir welds: although we can analyze material from a friction stir weld, we do not know the detailed thermomechanical history at specific points within a weld. This is because the metallurgical state can change radically with position due to the extreme thermal and strain field gradients within a friction stir weld. By contrast, the Gleeble allows us to generate a larger amount of material with a known thermomechanical history that we can test and evaluate. Furthermore, it allows us to independently vary strain and temperature with time in ways that may not even be possible under normal friction stir welding conditions.

At Carderock, we have independently varied temperature and strain on HSLA-65 material [1, 5] and on Nickel Aluminum Bronze [6]. In our study of Gleeble compression samples we found it beneficial to analyze the compression test with a numerical model because the strain field is not perfectly uniform due to minor barreling of the specimen (Figure 1). This numerical analysis provided a more accurate assessment of the actual strains experienced by the microstructures we analyze.
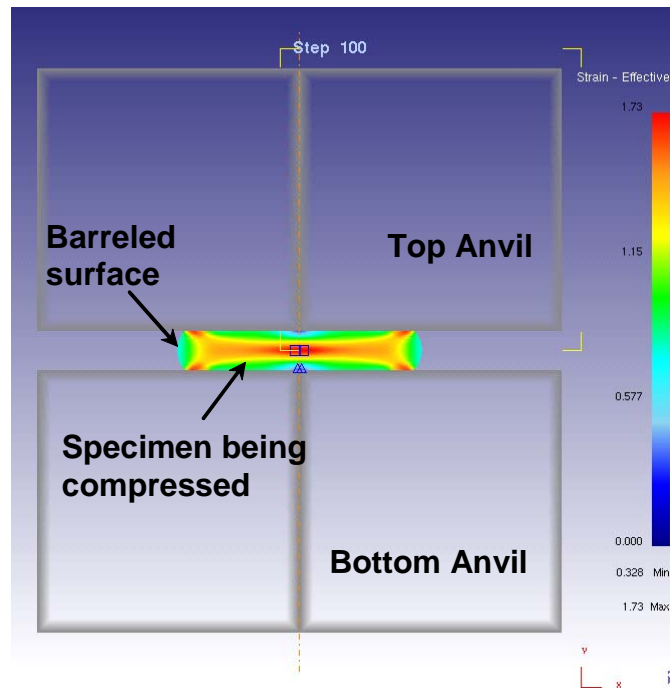

Figure 1   Longitudinal cross section of a cylindrical steel Gleeble specimen during deformation. This DEFORM 2D numerical analysis illustrates the spatial variation in effective strain during plastic deformation.

At Ohio State University Matthew Sinfield's master's thesis work [7] involved the use of a Gleeble 3800 Torsion machine on AISI 304L and HSLA-65 steels to simulate the friction stir welding of these materials. A photograph of the experimental setup is provided in Figure 2. We are now analyzing the OSU Gleeble torsion samples as part of an ILIR project to gain a fundamental understanding of microstructural evolution during friction stir welding of HSLA-65 steel for Naval applications [8, 9].

Any physical experiment that emulates the thermomechanical history in the deformation zone of a friction stir weld requires a highly dynamic test in terms of both deformation and temperature excursion, and the Gleeble torsion test is no exception. Because of the rapid temperature increase in the center of the sample prior to deformation, there is insufficient time for temperature to equilibrate along the entire test section. This results in a significant temperature gradient along the gauge length which in turn causes non-uniform deformation during the test (it twists more severely in the hottest—and therefore softest—regions of the gauge). Numerical modeling is a convenient tool to determine strains and strain rates in this complex system involving torsional metal flow along a temperature gradient. This method can provide a more accurate result than if one were to use the classical analytic equations [8, 10] that assume uniform flow stress throughout the test section.

This report describes the development of the DEFORM 3D model to simulate the Gleeble torsion test and calculate the spatial variations in strain and strain rate. This model is being used as part of the continuing ILIR project to relate different samples' microstructures and properties to their actual thermomechanical histories. That analysis will be presented in a separate, comprehensive report.

Procedure

First, we gathered constitutive data on the flow stress of HSLA-65 as functions of both temperature and strain rate. Then we found appropriate temperature-dependent thermophysical data on thermal expansion, thermal conductivity, and specific heat, and entered these into the model. We established the thermal boundary conditions based on experimental temperature measurements taken at three points on the test sample during test run #20 [7].

George Detraz (Code 6102) converted the engineering drawing of the test specimen into a 3D solid model in STL format, which can be imported directly into DEFORM 3D. Virtual chucks were created in order to hold one end and rotate the other end of the specimen.

The deformation of the workpiece was then modeled using elasto-plastic analysis with the Lagrangian reference frame, the sparse matrix solver, and the Newton-Raphson iteration method available within DEFORM 3D. The chucks were treated as rigid bodies.
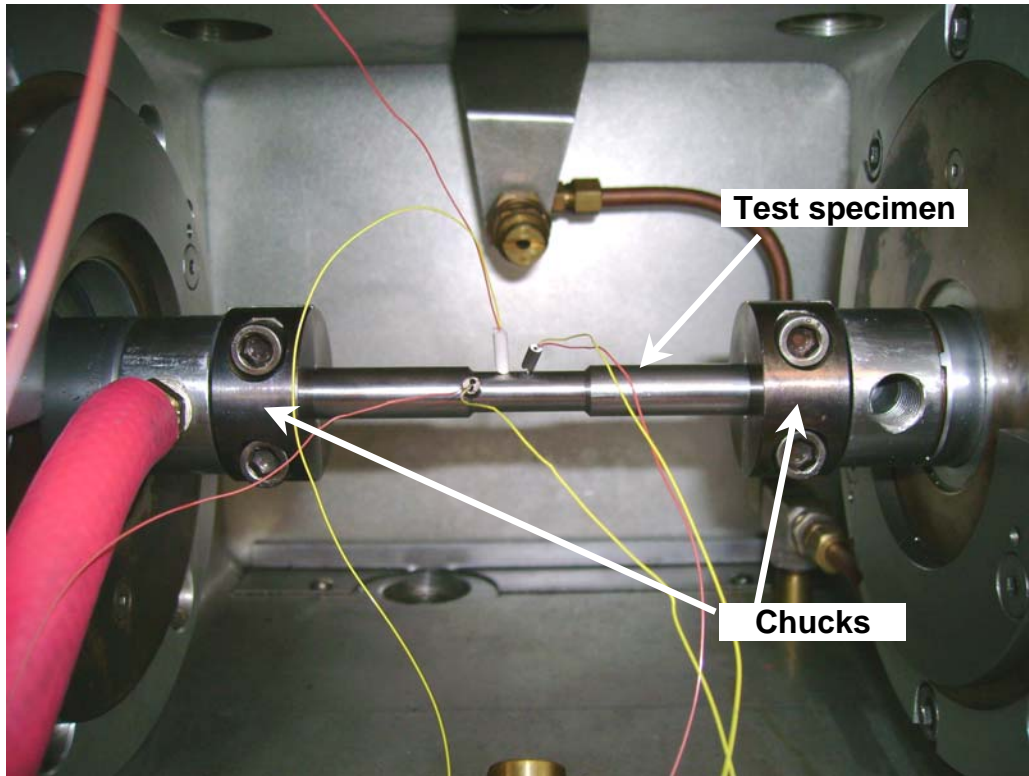
Figure 2   Experimental setup of Gleeble torsion test, showing thermocouple locations. The temperature of the sample is controlled by resistive heating from an applied current, with a feedback loop to a thermocouple. The chuck on the right is rotated rapidly so that the central (smaller diameter) gauge section with thermocouples is twisted. This is a hollow specimen with an outer diameter of 0.375" and an inner diameter of 0.188" at the center thermocouple location.

Constitutive Data

We relied on two principal sources of data for the constitutive behavior of the steel: HSLA-65 data developed by Nemat-Nasser for NSWCCD [11] and data provided by Dr. Chris Fisher (SFT, the DEFORM vendor) for a similar HSLA material (0.08% C, 1.3% Mn, 0.4% Si, 0.2% Ni, 0.08% V, 0.05% Nb) [12]. Although it is possible to use standard constitutive equations fitted to the data, we opted to incorporate the actual data into DEFORM 3D. The DEFORM software interpolates the data to calculate flow stress based on local temperature, strain, and strain rate at each nodal location in the system. One caveat with using this technique is that a complete data matrix must be provided. That is, the user must provide data at each of the independent variable levels they choose. In this case, we chose the temperatures, strains, and strain rates shown in Table 1, below.

Table 1. Summary of Data Levels Used in Constitutive Model
The Nemat-Nasser data levels that were available are highlighted in blue and the SFT data levels are highlighted in red. The plastic strain levels were arbitrarily chosen and interpolated from the available data.

Temperature (°C)	Plastic Strain (mm/mm)	Strain Rate (mm/mm/s)
23	0.0	0.001
327	0.1	0.1
427	0.2	1
527	0.3	10
727	0.4	100
900	0.5	3000
1000	10.0	
1100		
1200		
1370		

As shown in Table 1, there were 10 temperature levels x 7 plastic strain levels x 6 strain rate levels = 420 flow stress values provided in the dataset for DEFORM 3D. Because of lack of data as well as some inconsistencies between the two datasets, some values were interpolated, extrapolated, or adjusted as necessary to provide smooth, realistic behavior. The resulting curves are shown in Figures 3 thru 5.

These are not conventional stress-strain curves. Unlike in conventional true stress-true strain curves, the DEFORM curves require that there be a non-zero stress at zero strain. This is because these curves represent only the plastic deformation portion of stress-strain curves. At the onset of plastic strain (that is, zero plastic strain) there is a non-zero stress built up from the elastic deformation. For the Nemat-Nasser data, we offset the stress-strain curves by 0.02 to subtract out the elastic contribution to strain.

The high temperature, high strain rate (3000 s^{-1}) data are based on extrapolation (via multivariate regression analysis) of the data at other strain rates and temperatures and may, therefore, not be as accurate as the data for lower strain rates.

In DEFORM 3D the elastic portion of the stress strain curve is treated by providing the program with Young's Modulus for each temperature. These data were not available but were estimated from the room temperature modulus according to the curve in MIL-HDBK-5H [13]. They are plotted in Figure 6. Note that there is a significant extrapolation of the curve from 400°C to 1400°C. In the absence of data it is difficult to know how accurate the extrapolated high temperature values are, however elastic modulus data for stainless steels exhibit similar trends at the temperatures of interest [14].
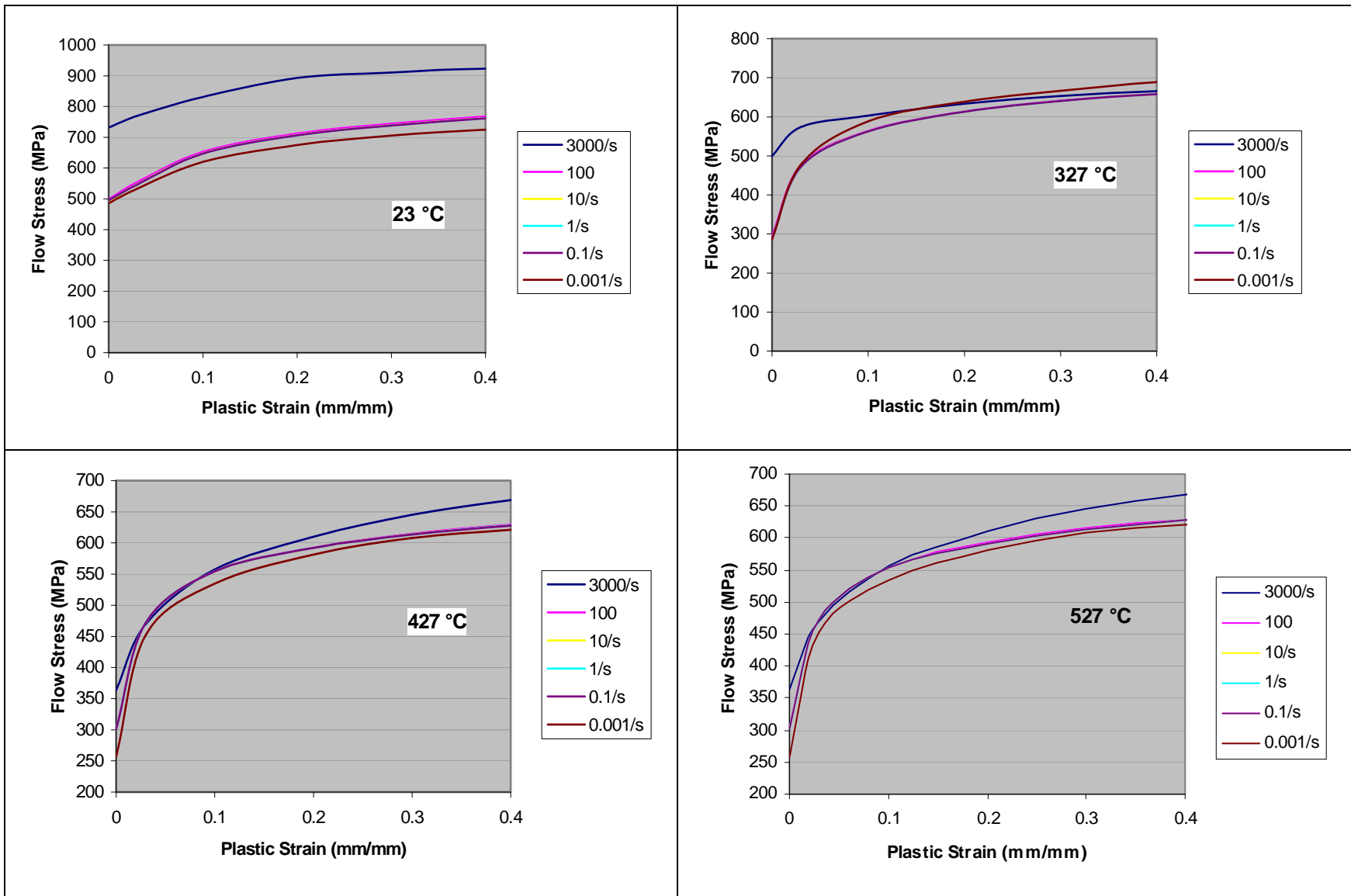
Figure 3 Flow stress at different plastic strains and strain rates. **These are not traditional stress strain curves.**
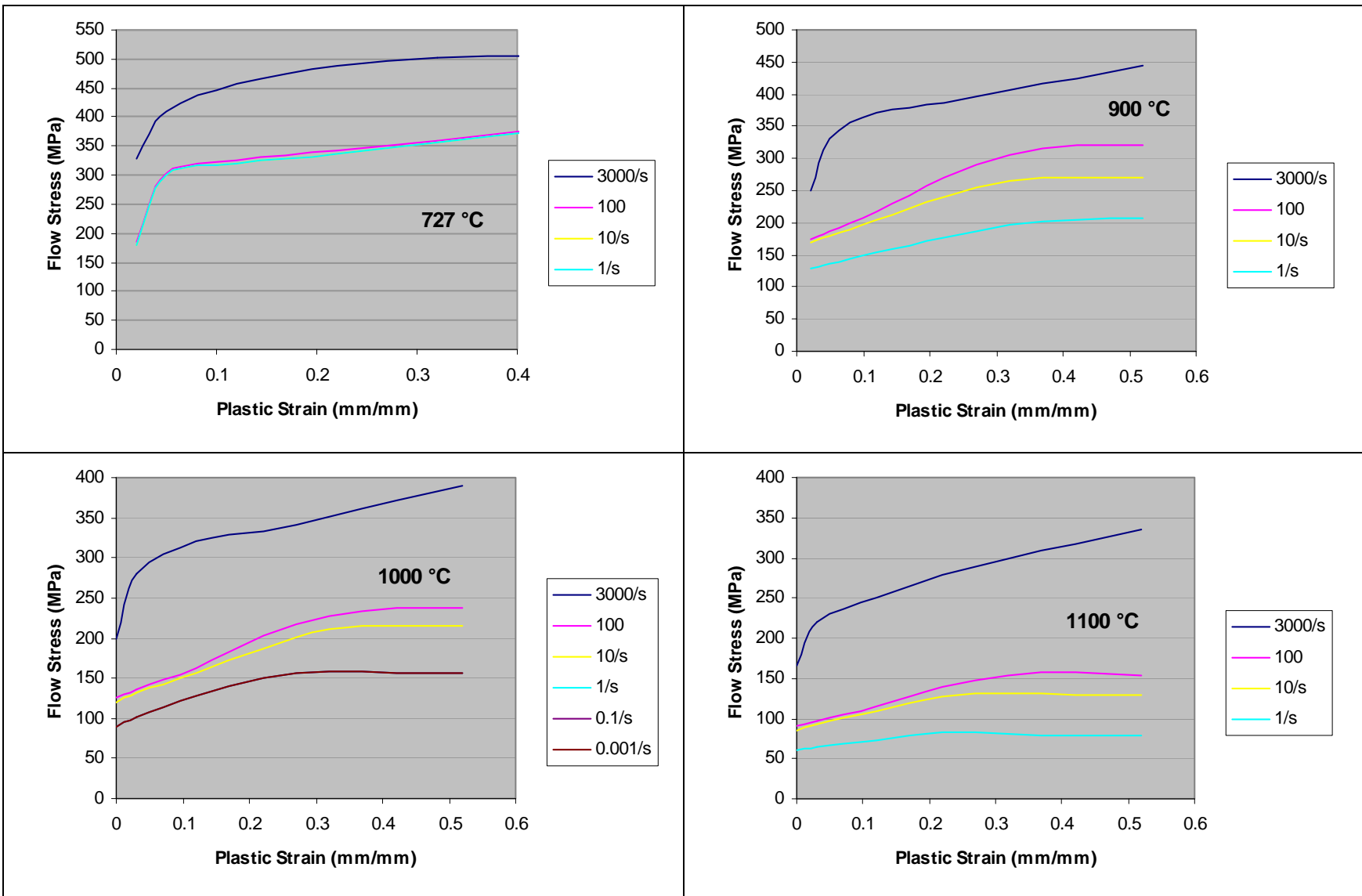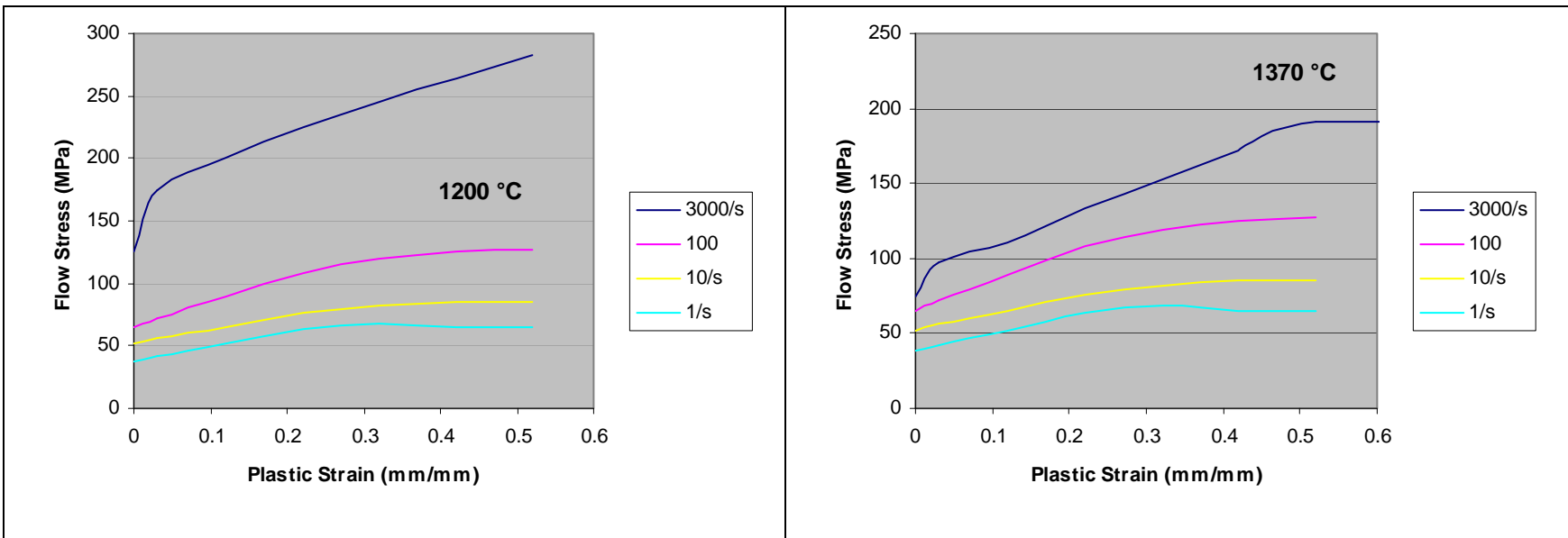
Figure 4   Flow stress at different plastic strains and strain rates. **These are not traditional stress strain curves.**

Figure 5   Flow stress at different plastic strains and strain rates. **These are not traditional stress strain curves.**
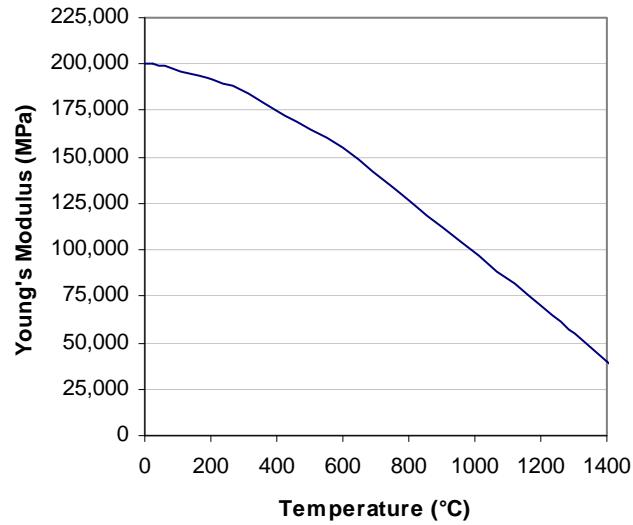
Figure 6   Temperature-dependent Young's Modulus data used in the elastic portion of the model.

Thermophysical properties

Temperature-dependent thermophysical properties (Fig. 7) were developed from sources in the literature for 1010 carbon steel [15], because these properties were not available for HSLA-65. The thermophysical properties are expected to be similar because the carbon content and other alloying elements are similar. DEFORM uses volumetric heat capacity rather than the more generally available specific heat. Volumetric heat capacity was calculated by taking the specific heat values (J/kg-K) at different temperatures and multiplying by density at those temperatures. The values also had to be converted to DEFORM's non-SI units of N/mm^2-°C.

Figure 7 Plots showing the temperature-dependent thermophysical properties employed by the model.

Meshing and Boundary Conditions

The solid CAD model of the test specimen was meshed with a triangular mesh of about 150,000 nodes as shown in Figure 8. Mesh windows were used to concentrate a finer mesh in the center of the sample where most of the deformation occurs.
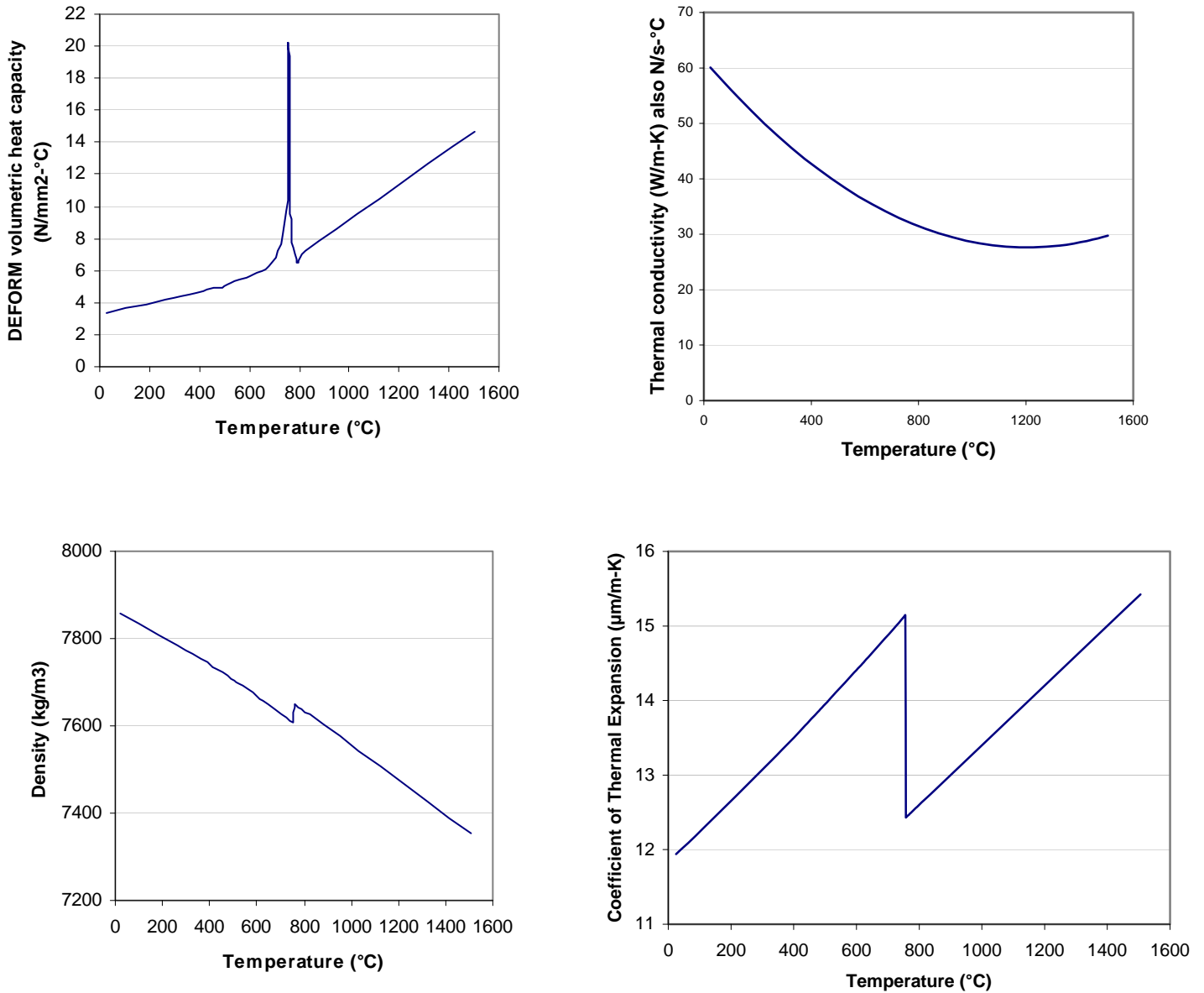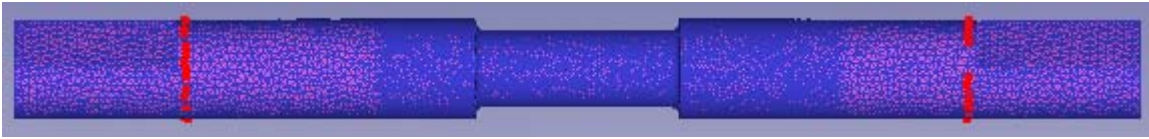
Figure 8   Finite element meshing scheme for the Gleeble torsion specimen. The nodes highlighted in red represent a constant temperature boundary condition of 400°C. Detailed boundary conditions for the gauge section are shown in Figure 9. A denser mesh can be seen in the central section of the specimen, where it is needed for more accurate calculation of the deformation.

In experimental Run 20 from Sinfield's master's thesis, temperatures were measured at three locations on the sample: at the center of the gauge length, 1/8" off-center, and at the end the gauge length next to the bevel or fillet [7]. A photograph of the experimental setup is provided in Figure 2. Because the measured temperatures remained fairly constant prior to and during the course of the deformation, the thermal problem was simplified by establishing constant temperature boundary conditions at the thermocouple locations as shown in Figures 8 and 9. We assumed that the specimen was thermally symmetric and we therefore duplicated the temperature boundary conditions with mirror symmetry. No heat transfer condition was specified between the workpiece and the chucks.
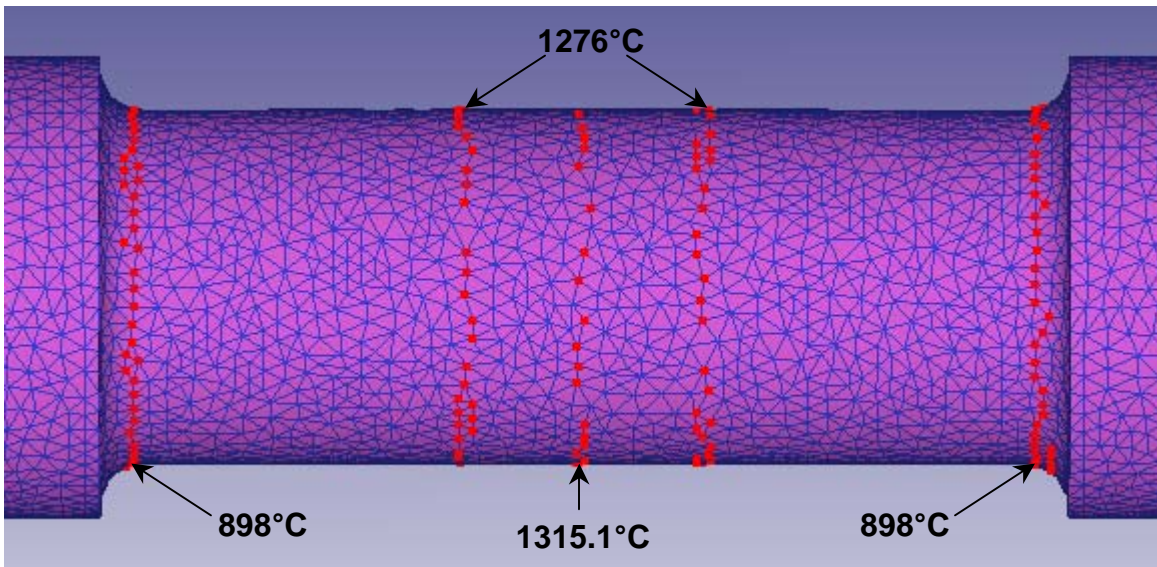

Figure 9   Detail showing constant temperature boundary conditions in the gauge section, corresponding to the thermocouple locations.

Friction

In this system, friction occurs between the chucks and the workpiece (at the flats on the ends of the torsion specimen). A coefficient of friction must be specified at the points of contact. We used a coefficient of friction value of 0.7, which is the system preset value for hot forging (dry).

Rotational motion

The deformation portion of the test occurred over a time interval of 0.1043 seconds for a single revolution of one end of the specimen. The speed was assumed to be constant, so a constant rotational velocity of 60.241 radians per second (575 rpm) was assigned to the chuck on the right side of the system shown in Figure 2. This condition exactly matches the programming of the Gleeble machine for Run 20. The problem was solved using 100 time steps (0.001043 seconds each). It took two days to perform the calculations on a dedicated modeling PC with a 2.66GHz Intel$^{®}$ Core 2 Duo E6700 processor and 2 Gb RAM.

Results

The results are presented below as a series of still images and links to the animations. In order for the animations to work, the electronic copy of this document must be accompanied by a folder entitled, "ANIMATIONS," which contains seven QuickTime files:

STRAIN_OVERVIEW.mov..Figure 10
STRAIN_SURFACE.mov..Figure 11
STRAIN_CUTAWAY.mov ....Figure 13
STRAIN_RATE_CUTAWAY.mov ....Figure 14
STRAIN_RATE_SURFACE.mov ....Figure 14
ISO_STRAIN_SURFACES.mov ....Figure 15
STRAIN_SURFACE_MULTI-POINT_TRACK.mov....Figure 16

An overview of the test, showing the specimen and chucks, is provided in Figure 10. The chuck on the right has been rotated counterclockwise one full revolution, resulting in a non-uniform distribution of strain in the gauge section. The strain distribution is seen in the color contour plot. The maximum strain was about 1.9 mm/mm in the center of the gauge section on the outer diameter.
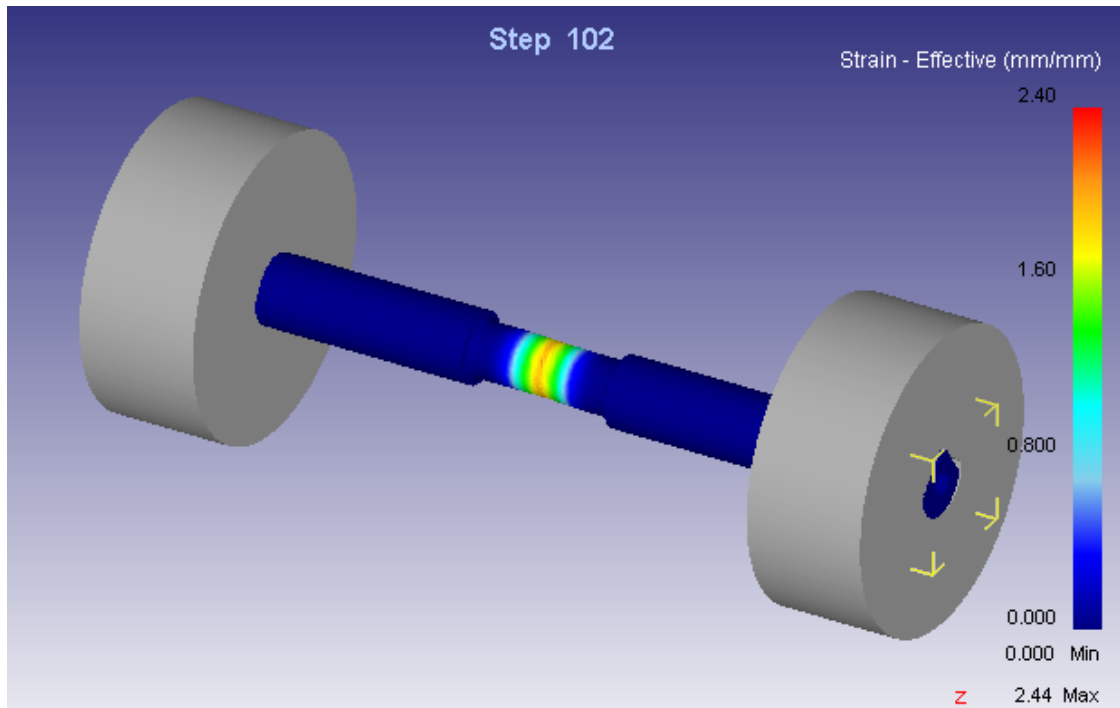
Figure 10 Overview of system showing strain distribution after one revolution.
Hyperlink to animation: STRAIN_OVERVIEW.mov

Figure 11 provides a detailed view of the strain evolution in the deformation region. The gauge length is 1" and the diameter is 3/8" in this region. The image clearly shows that deformation does not take place over the entire gauge length, but rather it is confined to about half the gauge length. Blindly solving the problem using available analytic equations would yield an incorrect result of a uniform distribution of strain over the full gauge length, because of the assumption of a uniform temperature distribution over the entire region.
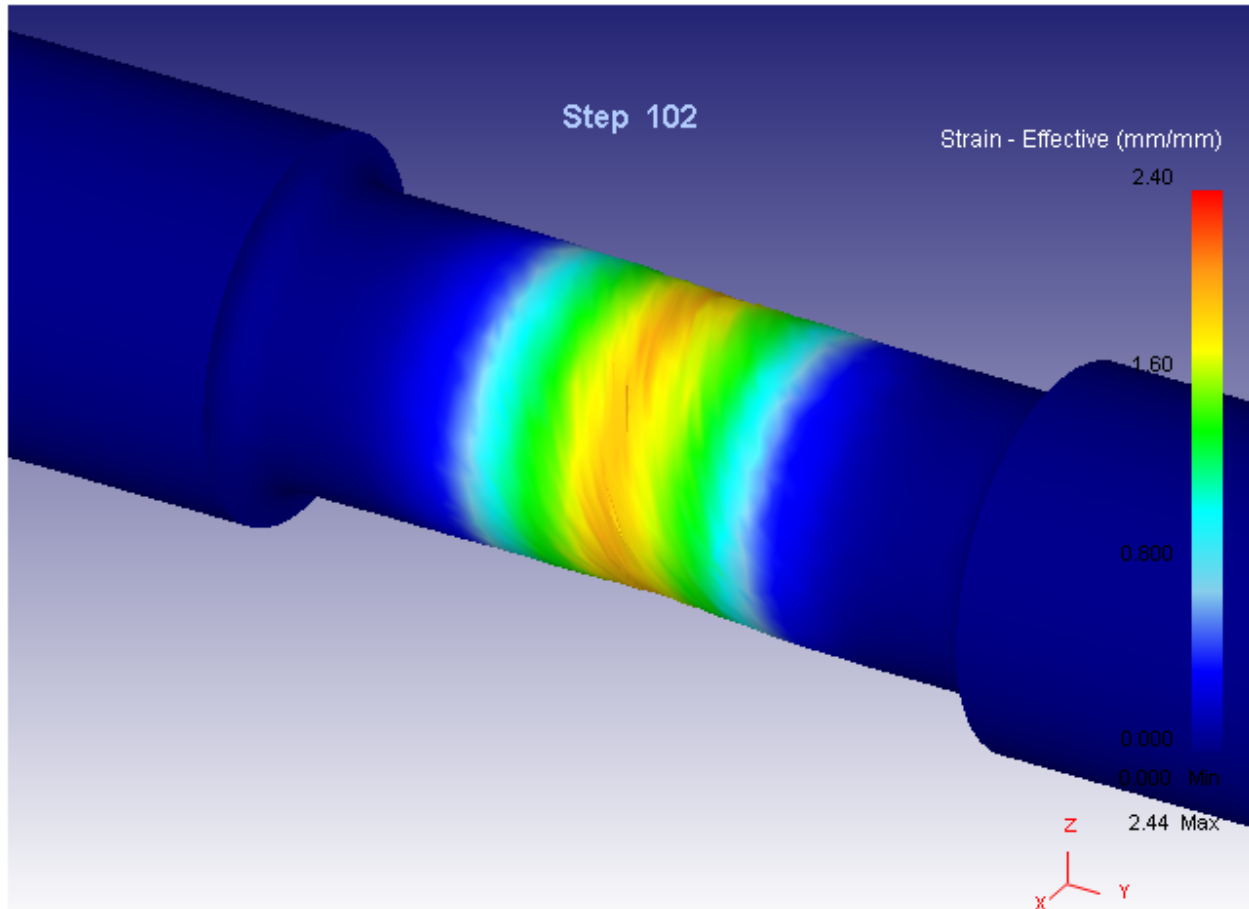

Figure 11   Detailed view showing strain distribution in gauge section after one revolution.
Hyperlink to animation: STRAIN_SURFACE.mov

Figure 12 provides a detailed view of the temperature field in the deformation region. It is this temperature gradient that causes the metal to flow more readily in the center of the specimen than at the edges of the gauge length. As in the actual Gleeble torsion test, the temperature field was first solved in the simulation to provide a converged initial condition, then the deformation portion of the simulation was run (maintaining the temperature field during the simulation). The temperatures were based on experimentally measured values, which varied negligibly during the deformation. Because the constant temperature boundary conditions do not vary with time, this is a steady state solution.
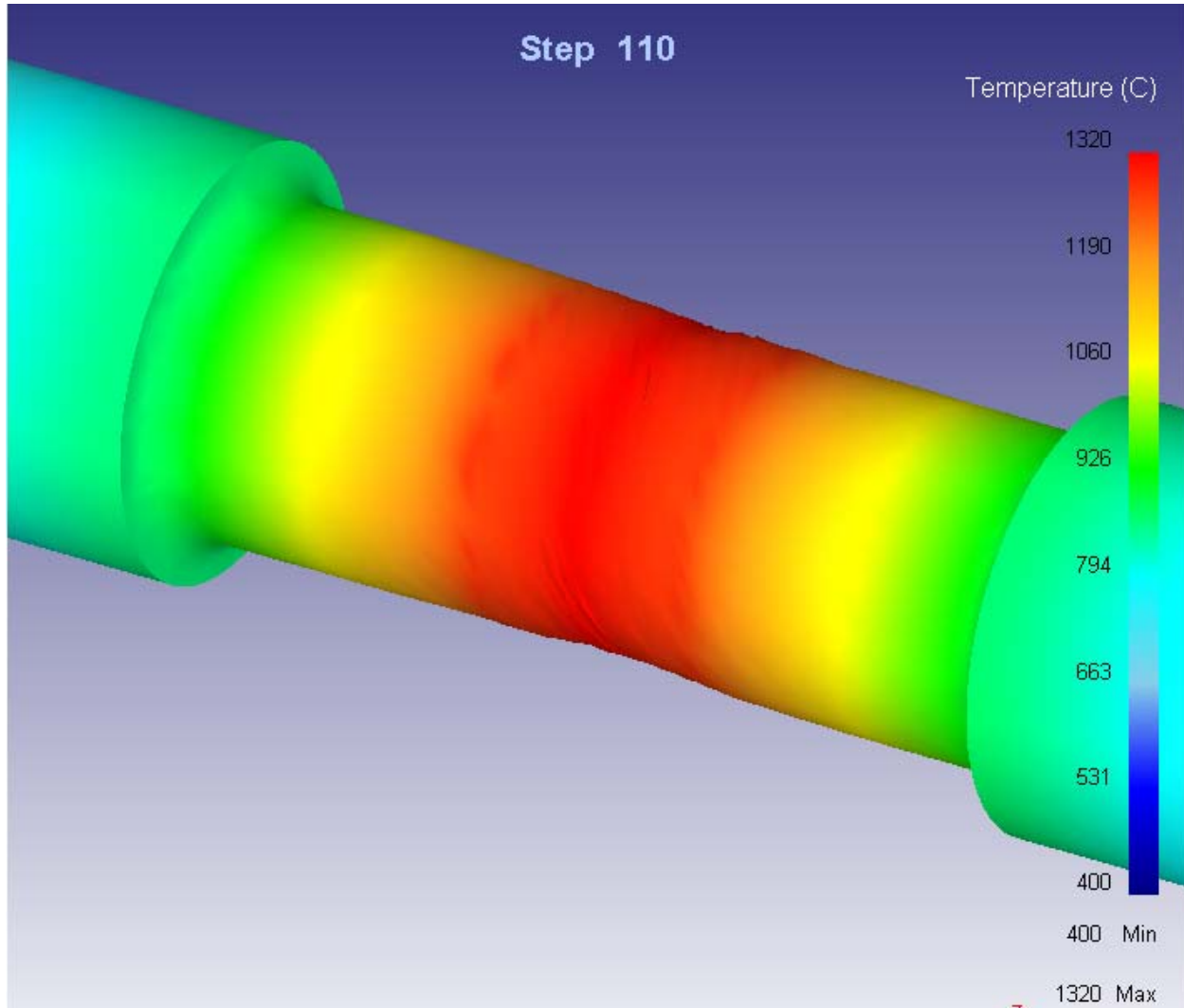

Figure 12   Contour plot showing the steady state temperature field after deformation.

Figure 13 provides a cutaway view, showing the variation in strain evolution through the thickness of the torsion sample (at the center of the gauge length). The amount of strain varies significantly according to both radius and axial position. In this cutaway plane, the maximum strain at the outer radius is 1.9 mm/mm and the strain at the inner radius is about 0.8 mm/mm. The model provides us with critical data on the thermomechanical history at each point in the cross section to correlate with the hardness and microstructure measurements.

While the reader should keep in mind that the surface texture seen in Figure 13 is a numerical artifact of the mesh refinement and use of a Lagrangian reference frame, it is anecdotally true that the actual test specimens had a similar surface texture appearance after deformation (in addition to a classic orange peel pattern).
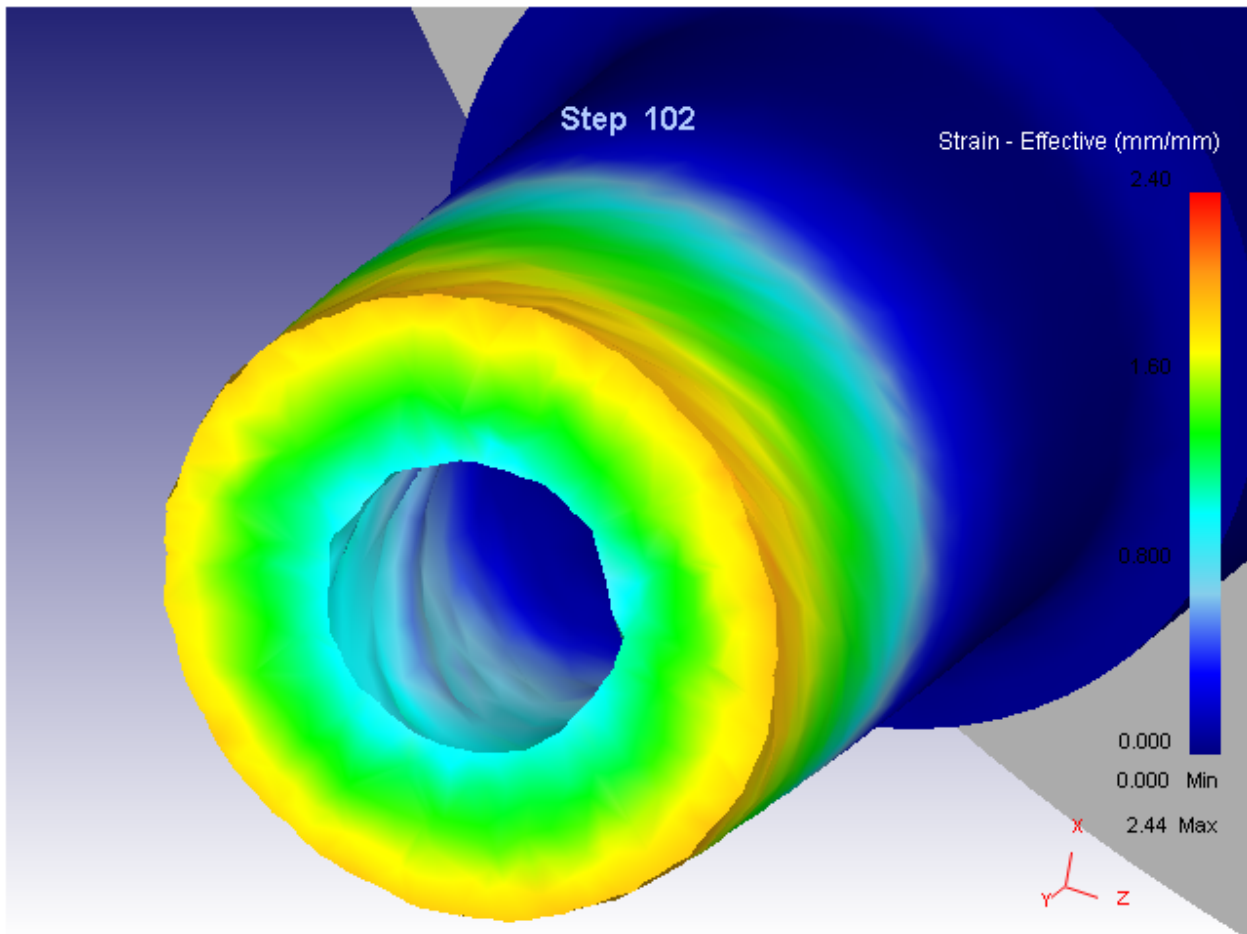
Figure 13   Distribution of effective strain seen in transverse cutaway view
through center of the gauge after testing.
Hyperlink to animation: STRAIN_TRANSVERSE _CUTAWAY.mov

Although the rotational velocity of the drive chuck is constant, the strain rate is _neither constant nor uniform_ during this test. Figure 14 shows the spatial variation in effective strain rate, and the animations reveals how strain rate changes throughout the specimen during the

course of the test. Note that these animations were generated with a slightly different mesh than the other animations. This resulted in the simulated sample deforming in a slightly different manner, although the calculated strains are nearly identical. The bend in the gauge section is more prominent with this mesh than with the others.
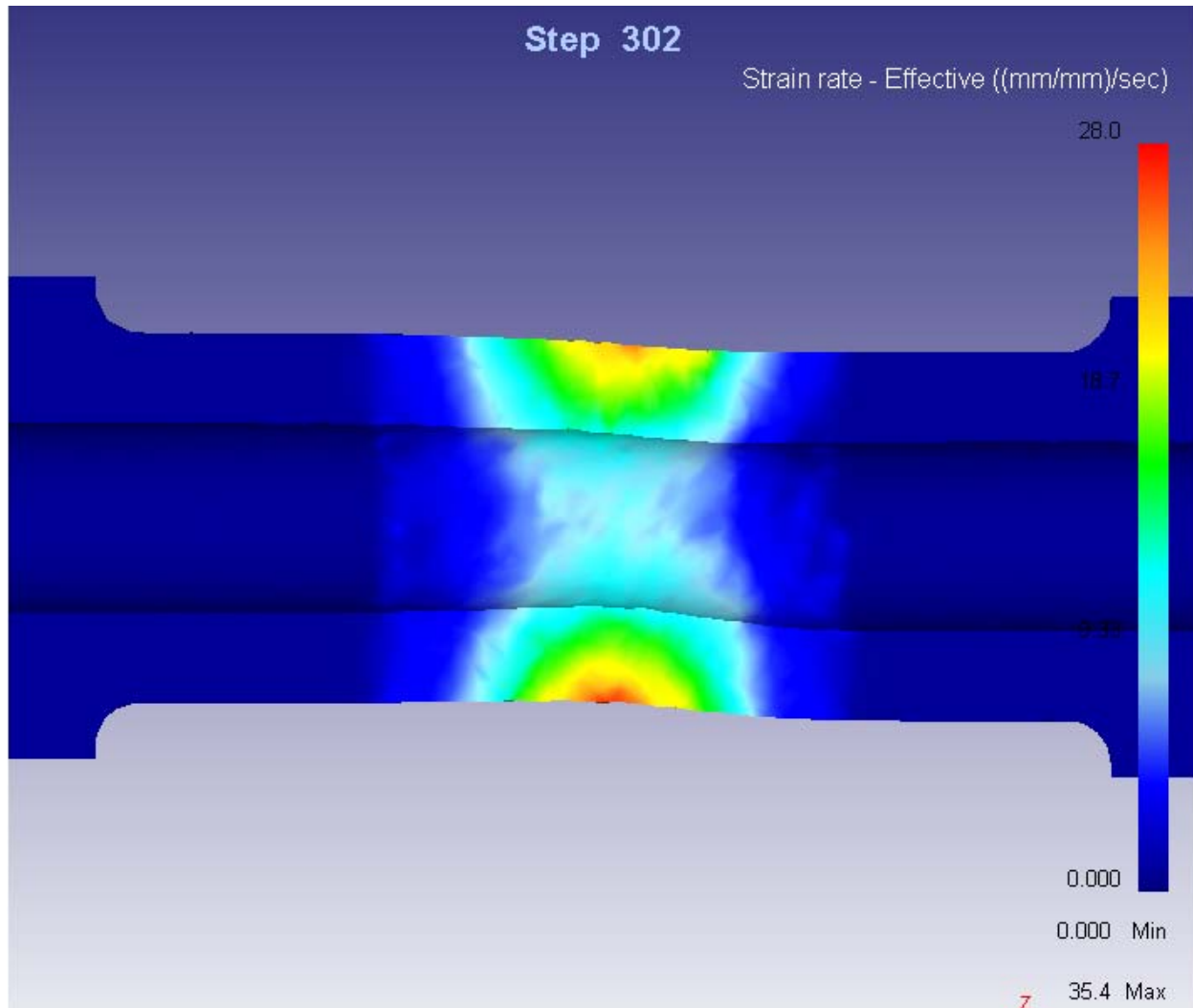

Figure 14 Spatial variation of strain rate within the sample at the end of the deformation.

Hyperlink to animation showing temporal variation in strain rate on the surface: STRAIN_RATE_SURFACE.mov

Hyperlink to animation showing temporal variation in strain rate through the cross section: STRAIN_RATE_CUTAWAY.mov

Iso-strain contours provide a unique insight into the behavior of metal flow during the test. In Figure 15, the dark blue surfaces, which are the first to appear, are the surfaces at which the strain is zero—all points outside of these surfaces, away from the center, also have zero strain. Increasingly higher strains are continually generated in the center of the gauge length, on the OD surface, then those iso-strain surfaces move toward the sample ends and sink radially inward as the test progresses, creating a striking visual effect in the animation.
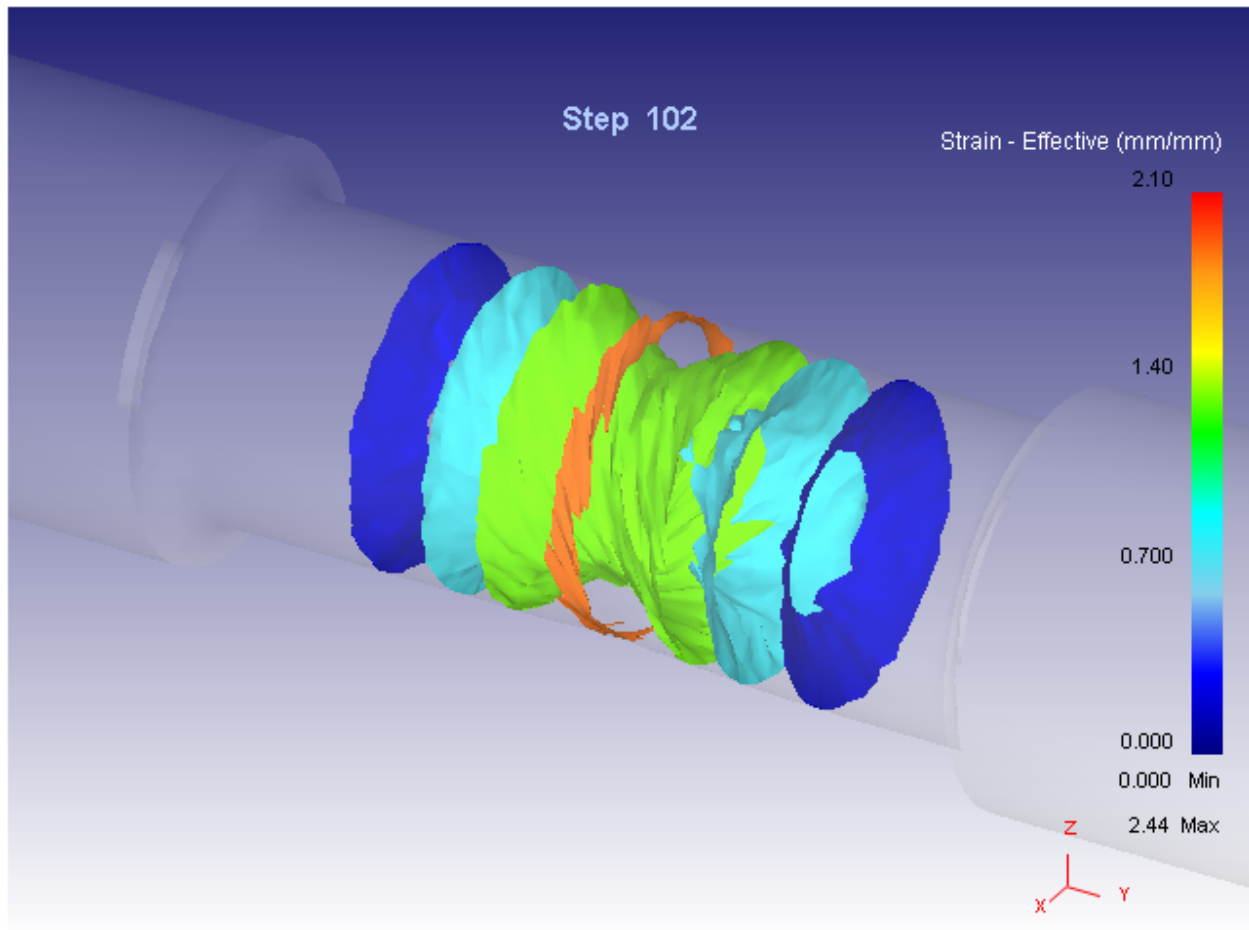
Figure 15   Iso-strain surfaces within the sample show that increasingly higher strains are generated on a central ring in the middle of the sample, then move outward toward the sample ends.

Hyperlink to animation: ISO-STRAIN_SURFACES.mov

The point tracking feature provides quantitative information at points of interest in the sample. The surface points shown in Figure 16 started as a straight line of points at the top of the sample, and rotated to different positions after one revolution of the chuck. The point in the center of the gauge length accumulated an effective strain of 1.86 mm/mm.

Figure 16 Point tracking provides quantitative information at points of interest. **Hyperlink to animation: STRAIN_SURFACE_MULTI-POINT_TRACK.mov**

Validation of the Model

Use of the metric 'angle of twist along gauge length after deformation' is a reasonable test of the model's ability to correctly predict deformation behavior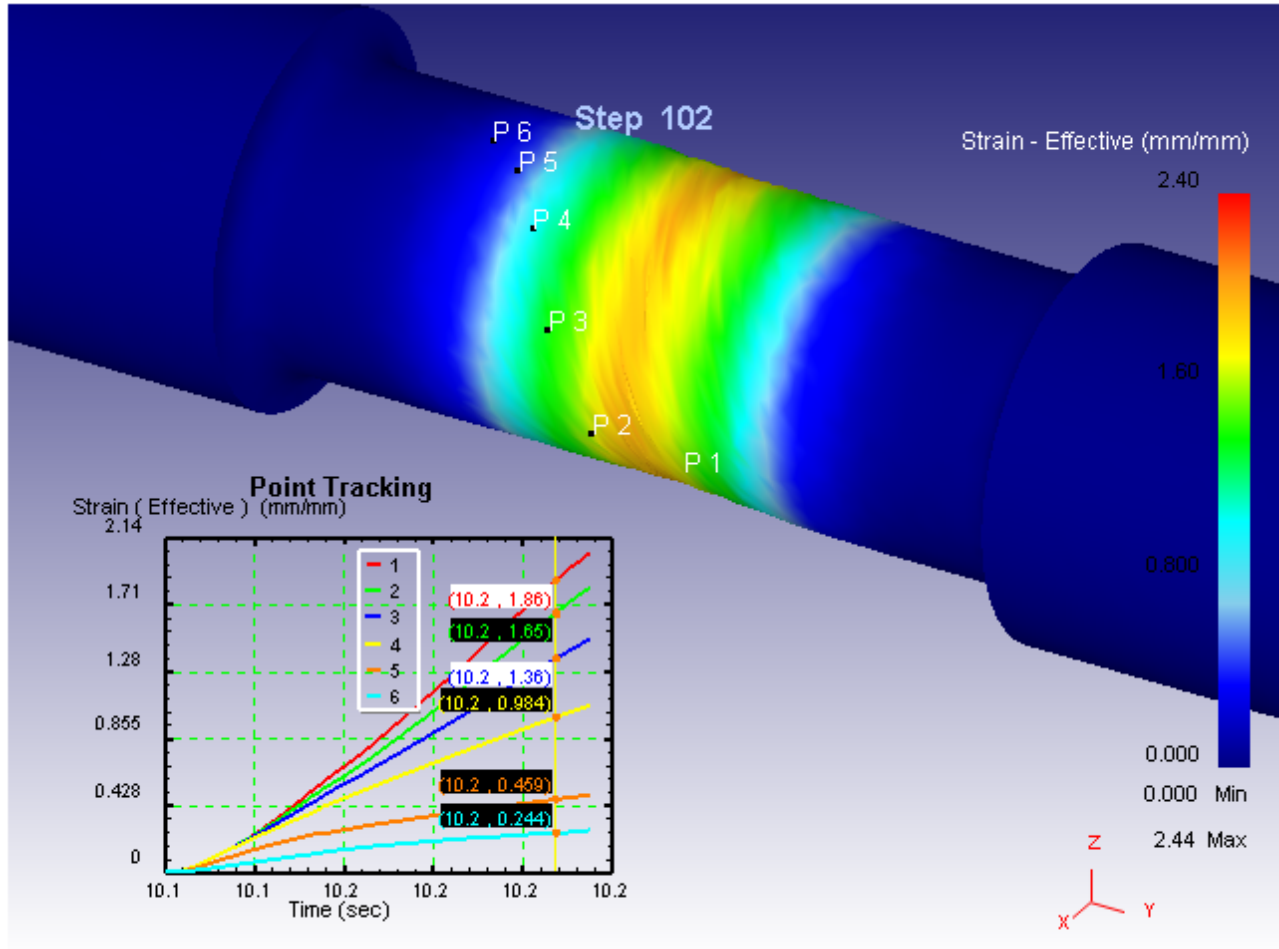. We compared experimental measurements of surface deformation to the model's predictions (see Figure 17). The results show good agreement between experimental measurements and numerical predictions.

Potential sources of error. The experimental measurements excluded elastic springback of the sample at the deformation temperatures.[1] However, this only made a minor difference in the measured values, with a maximum error of 2° at the end of the gauge length. The numerical simulation predicted that the drive side of the sample whould shift off-axis (i.e., buckle) a maximum of 0.9mm during testing. The extent of buckling in the actual sample is unknown. The numerical simulation angle of twist measurements accounted for the shifted geometric center, but the experimental measurements may have been non-uniformly influenced by any sample distortion. The quality of the numerical simulation is directly related to the quality of the constitutive data; better high temperature data could improve the agreement with experimental measurements.
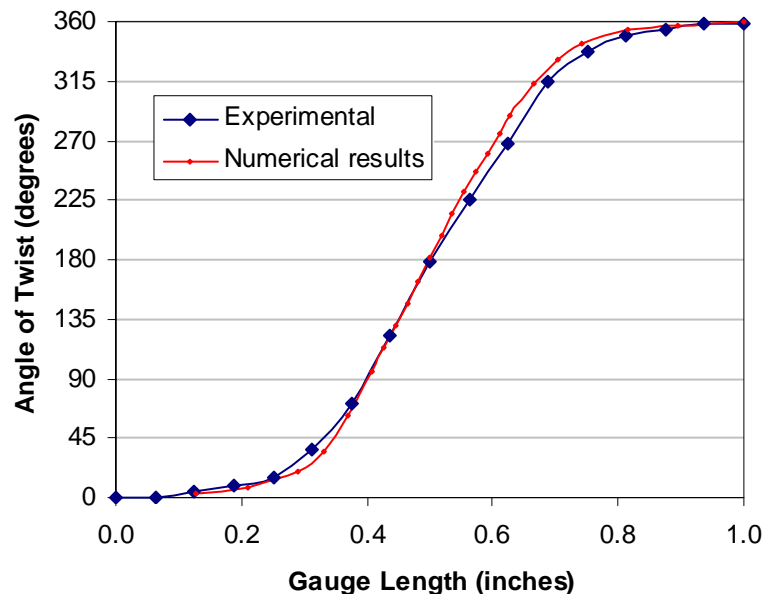
Figure 17 Graph comparing predicted versus actual surface deformation.

---

[1] Before experimental testing, a straight line was scribed on the surface of the gauge length from shoulder to shoulder (fixed to rotated end). After testing, the sample was removed from the Gleeble chucks and a new straight line was scribed in place of the original, starting from the fixed end shoulder to the rotated end. The scribed line was used as a quantifiable measure of angular deflection against the superimposed "original line." In all torsion samples the new scribed lines never reached the original lines' end points at the rotated end shoulder. This resulted in the angle of twist at the rotated sample end to not be equal to 360°, but slightly less. The "incomplete" rotation was attributed to the relaxation of elastic strain built in the system as the sample was removed from the Gleeble torsion chucks, or "springback."

Conclusions and Recommendations

We developed a numerical model of a Gleeble torsion test that predicts the deformation behavior of a specimen to a high degree of fidelity, and provides detailed quantitative information about the strain, strain rate, and temperature history with time throughout the volume of the specimen. The torsion test had been performed as a physical experiment to model the friction stir welding of HSLA-65 steel. However, the numerical model was necessary to determine the complex thermomechanical distribution within the sample, in order to interpret the test results. The numerical model is being used as part of the continuing ILIR project to relate different torsion sample microstructures and properties to their actual thermomechanical histories for comparison with actual friction stir welds.

Another benefit of this work is that we now have a material model for the high temperature deformation of HSLA-65 that can be used for future DEFORM simulations. For example, we can use DEFORM 3D to model the friction stir welding process itself, accounting for many of the physical effects that are not taken into account by our current friction stir model [16].

References

[1]   D. R. Forrest, et al., "Simulation of HSLA-65 Friction Stir Welding," Trends in Welding 2005, ASM International, Proceedings of the 7th International Conference on Trends in Welding, held 16-20 May 2005, Pine Mountain, GA.

[2]   D. Forrest and M. Posada, "Friction Stir Welding of HSLA-65," FY04 Annual progress report to ONR, Contract No. N00014-04-WX-2-0548, 20 September 2004.

[3]   D. Forrest and M. Posada, "Friction Stir Welding of HSLA-65," FY05 Annual progress report to ONR, Contract No. N00014-05-WX-2-0503, 25 October 2005.

[4]   D. Forrest and M. Posada, "Friction Stir Welding of HSLA-65," FY06 Annual progress report to ONR, Contract No. N00014-06-WX-2-0453, 8 September 2006.

[5]   D. Forrest and M. Posada, "Friction Stir Welding of HSLA-65 for Naval Shipbuilding," FY07 Annual progress report to ONR, Contract No. N00014-07-WX-2-0221, 25 September 2007.

[6]   F. A. Pierce, "The Isothermal Deformation of Nickel Aluminum Bronze in Relation to Friction Stir Processing," Master's thesis, Naval Postgraduate School, June 2004.

[7]   M. F. Sinfield, "Advancements in Physical Simulation and Thermal History Acquisition Techniques for Ferrous Alloy Friction Stir Welding," Master's thesis, Ohio State University, 2007.

[8]   M. Posada, "A Study on How Metallurgical Factors are Affected by the Solid-State Stirring Nature of Friction Stir Welding," ILIR proposal, Naval Surface Warfare Center Carderock Division, 1 June 2005.

[9]   Sinfield, et al., "Physical Simulation of Friction Stir Weld Mictrstructures of a High Strength, Low Alloy Steel (HSLA-65)," Proceedings of the TWI 7th International FSW Symposium, held 20-22 May 2008, Awaji Island, Japan.

[10]   S. L. Semiatin and J. H. Holbrook, "Plastic Flow Phenomenology of 304L Stainless Steel," Met. Trans. A, 14A, p. 1681-1695 (August 1983).

[11]   S. Nemat-Nasser and Wei-Guo Guo, "Thermomechanical Response of HSLA-65 Steel Plates: Experiments and Modeling," unpublished, 19 June 2003.

[12]   Data file used by permission from Scientific Forming Technologies: data from Prasad, "Hot Working Guide;" extended using equations from Doege, "Fleisskurven-Atlas."

[13]   Military Handbook: Metallic Materials and Elements for Aerospace Vehicle Structures, MIL-HDBK-5H, United States Department of Defense, Figure 9.3.1.3, page 9-68, 1 December 1998.

[14]   *Source Book on Materials for Elevated Temperature Applications*, *ed*. Elihu F. Bradley, American Society for Metals, Metals Park, OH, Table 7, p. 193, 1979.

[15]   *Metals Handbook*, 9th edition, v. 1, Properties and Selection: Irons and Steels, American Society for Metals, Metals Park, OH, p. 146-149.

[16]   D. R. Forrest, "Evaluation and Application of the Boeing Model for Numerical Simulation of Friction Stir Processing," NSWCCD-61-TR-2006/08, May 2006.

Distribution

CONUS - DoD	copies	INTERNAL		copies
OFFICE OF NAVAL RESEARCH		0120	(BARKYOUMB)	1
ONR 33 (J. CHRISTODOULOU)	1	60		1
875 NORTH RANDOLPH ST.		61		1
SUITE 1425		6101		1
ARLINGTON VA 22203-1995		6102		1
		611		1
OFFICE OF NAVAL RESEARCH		611	(FORREST	1
ONR 33 (FONDA)	1	611	(SINFIELD)	1
875 NORTH RANDOLPH ST.		611	(DAVIS)	1
SUITE 1425		611	(POSADA)	1
ARLINGTON VA 22203-1995		611	(WOLK)	1
		612		1
COMMANDER		613		1
NAVAL SEA SYSTEMS COMMAND		614		1
SEA 05P24	1	615		1
1333 ISAAC HULL AVENUE SE		616		1
WASHINGTON DC 20376		617		1
		63	(REPT DOCUMENTATION PG)	1
DEFENSE TECHNICAL	1	65		1
INFORMATION CENTER		652	(Y. HWANG)	1
727 JOHN J KINGMAN ROAD		66	(REPT DOCUMENTATION PG)	1
SUITE 0944		6550	(RULE)	1
FORT BELVOIR VA 22060-6218		3442	(TIC - PDF ONLY)	1

This page intentionally left blank